Recruitment of HIF-1α and HIF-2α to common target genes is differentially regulated in neuroblastoma: HIF-2α promotes an aggressive phenotype

Linda Holmquist-Mengelbier,[1,5] Erik Fredlund,[1,5] Tobias Löfstedt,[1] Rosa Noguera,[2] Samuel Navarro,[2] Helén Nilsson,[1] Alexander Pietras,[1] Johan Vallon-Christersson,[3] Åke Borg,[3] Katarina Gradin,[4] Lorenz Poellinger,[4] and Sven Påhlman[1,*]

[1] Division of Molecular Medicine, Department of Laboratory Medicine, Lund University, University Hospital MAS, SE-205 02 Malmö, Sweden
[2] Department of Pathology, University of Valencia, Medical School, Valencia, Avda Blasco Ibañez 17, 46010 Valencia, Spain
[3] Department of Oncology, Lund University, SE-221 00 Lund, Sweden
[4] Department of Cell and Molecular Biology, Medical Nobel Institute, Karolinska Institute, SE-171 77 Stockholm, Sweden
[5] These authors contributed equally to this work.
*Correspondence: sven.pahlman@med.lu.se

Summary

In neuroblastoma specimens, HIF-2α but not HIF-1α is strongly expressed in well-vascularized areas. In vitro, HIF-2α protein was stabilized at 5% O_2 (resembling end capillary oxygen conditions) and, in contrast to the low HIF-1α activity at this oxygen level, actively transcribed genes like VEGF. Under hypoxia (1% O_2), HIF-1α was transiently stabilized and primarily mediated acute responses, whereas HIF-2α protein gradually accumulated and governed prolonged hypoxic gene activation. Knockdown of HIF-2α reduced growth of neuroblastoma tumors in athymic mice. Furthermore, high HIF-2α protein levels were correlated with advanced clinical stage and high VEGF expression and predicted poor prognosis in a clinical neuroblastoma material. Our results demonstrate the relevance of HIF-2α in neuroblastoma progression and have general tumor biological implications.

Introduction

The oxygen pressure within solid tumors is heterogeneous, ranging from approximately 5% O_2 in well-vascularized regions to anoxia near necrotic regions, but is on average in the hypoxic range (about 1% O_2) (Brown and Wilson, 2004; Goda et al., 1997; Höckel and Vaupel, 2001). In response to hypoxia, tumor cells adapt by changing the transcription of genes involved in angiogenesis, cell survival, and metabolism. The hypoxia-inducible transcription factors HIF-1α and HIF-2α are critical for this adaptive response (Harris, 2002; Semenza, 2003). At hypoxia the α subunits are stabilized, heterodimerize with the constitutively present partner HIF-1β/ARNT, and together with coactivators such as CBP/p300 regulate genes via specific hypoxia response elements (HREs) (Semenza, 2003). In the presence of oxygen, prolyl hydroxylases (PHDs) modify the HIF-α proteins at two conserved prolines, resulting in HIF interaction with the von Hippel-Lindau (VHL)-E3 ligase protein complex, targeting HIFs for ubiquitylation and subsequent proteasomal degradation (Epstein et al., 2001; Huang et al., 1998; Kallio et al., 1999). HIF transcriptional activity is further regulated by an oxygen-dependent asparagyl hydroxylase, FIH-1 (factor inhibiting HIF) leading to reduced interaction with CBP/p300 coactivators (Lando et al., 2002; Mahon et al., 2001). In addition to hypoxia, HIF-1α protein synthesis, stability, and activity can also be regulated by other mechanisms, for instance, in response to growth factor-induced signaling (Semenza, 2003).

There are several known and well-characterized HIF-1α target genes (Semenza, 2003; Wenger et al., 2005), whereas no exclusive HIF-2α target gene has yet been identified, with the possible exception of the recently reported Oct-4 (Covello et al., 2006). There is a redundancy regarding HIF targets (Sowter et al.,

SIGNIFICANCE

Mechanisms for efficient cellular adjustment to oxygen shortage probably evolved in parallel to development of oxygen-dependent multiorgan organisms. The hypoxic response through HIF transcription factors results in phenotypic changes much resembling those of neoplastic progression. Generally, tumor hypoxia/presence of HIF-1α protein correlates with poor prognosis. The presence of HIF-2α in well-vascularized neuroblastomas correlates with VEGF expression and unfavorable patient outcome. Moreover, the observation that HIF-2α regulates classical hypoxia-driven genes (such as VEGF) at end capillary O_2 levels indicates that HIF-2α can act oncogenically, independently of a hypoxic environment. The present data also suggest differential utilization of HIF proteins in neuroblastoma cells at acute versus prolonged hypoxia, which could have significant implications for the design of anti-HIF therapy in tumor disease.

2003); however, it has been reported that these two factors display some differences in their preference for the genes they regulate. For example, glycolytic enzymes are suggested to be preferentially targeted by HIF-1α (Hu et al., 2003; Wang et al., 2005), whereas HIF-2α appears to regulate the expression of *MT1-MMP* (Petrella et al., 2005), *EPO* (Warnecke et al., 2004), and *PAI-1* (Sato et al., 2004), although these genes are regulated by HIF-1α as well (Semenza, 2003). *HIF-1α* expression is found in most cell types (Jain et al., 1998), and *hif-1α*$^{-/-}$ mice die at approximately embryonal day 11 (E11) with neural tube defects and cardiovascular malformations, reflecting the importance of HIF-1α during development (Iyer et al., 1998; Ryan et al., 1998). *HIF-2α* is highly expressed in vascular structures (Jain et al., 1998) but also in distinct cell populations of most organs, including brain, heart, lung, kidney, and liver (Wiesener et al., 2003). During embryogenesis, HIF-2α protein is selectively expressed during short, discrete time periods in different parts of the developing murine and human sympathetic nervous system (SNS) (Jögi et al., 2002; Nilsson et al., 2005; Tian et al., 1998), and a role in normal SNS development has been proposed (Tian et al., 1998). In *hif-2α*$^{-/-}$ mice, reduced catecholamine synthesis (Tian et al., 1998) and severe vascular defects (Peng et al., 2000) have been demonstrated. HIF-1α and HIF-2α have also been implicated in tumorigenesis (Harris, 2002; Semenza, 2003) and are frequently coexpressed in human tumors (Talks et al., 2000).

The childhood tumor neuroblastoma is derived from SNS precursor cells or immature SNS neuroblasts (Hoehner et al., 1996). We have previously shown that neuroblastoma cells respond to low oxygen by induction of a hypoxic phenotype and that hypoxic neuroblastoma cells become dedifferentiated and gain SNS stem cell characteristics (Jögi et al., 2002, 2004), features that in the clinical setting are associated with increased aggressiveness and adverse patient outcome (Wei et al., 2004). Here we report that neuroblastoma specimens frequently have strong expression of HIF-2α protein in well-vascularized tumor areas. In vitro, HIF-2α, as opposed to HIF-1α protein, is strongly induced at physiological oxygen concentrations (5% O_2). Furthermore, under chronic hypoxia (1% O_2) HIF-1α protein is degraded over time, whereas HIF-2α is continuously accumulated. Global gene expression analysis revealed genes closely following the HIF stabilization patterns at 1% and 5% O_2. HIF subcellular localization and genomic DNA binding, together with specific HIF knockdown, indicated a temporally regulated mode of HIF utilization during cellular adaptation to hypoxia, where HIF-1α primarily mediates fast (acute) and HIF-2α mediates late (chronic) responses to hypoxia. In addition, expression of known hypoxia-driven genes were induced in a HIF-2α-dependent manner at 5% O_2, indicating a role of HIF-2α in promotion of an aggressive neuroblastoma phenotype at physiological as well as chronic hypoxic oxygen levels. Accordingly, transient knockdown of HIF-2α reduced growth of xenografted neuroblastoma tumors in athymic mice. Immunohistochemical evaluation of a clinical neuroblastoma tumor material further demonstrated a significant correlation between HIF-2α and VEGF protein levels, and a strong and significant correlation between high HIF-2α protein content and unfavorable patient outcome was found. Taken together, these data clearly implicate HIF-2α as an important factor determining neuroblastoma aggressiveness, and HIF-2α could therefore represent an important target in neuroblastoma therapy.

Results

HIF-1α and HIF-2α induction patterns differ in neuroblastoma cells

We immunostained consecutive sections of neuroblastoma specimens for HIF proteins and the blood vessel endothelial marker CD31. We consistently (18/20 tumors) found weak to strong HIF-2α immunoreactivity in tumor cells adjacent to blood vessels (Figures 1A–1B), while HIF-1α staining in vascularized areas was negative (data not shown). Importantly, the HIF-2α protein was frequently localized to nuclei, consistent with functional activity also in well-vascularized lesions. These observations prompted us to analyze in closer detail the kinetics by which HIF protein levels and functions change in cultured neuroblastoma cells at different oxygen levels. At 1% O_2, HIF-1α levels were rapidly induced to peak within hours and thereafter gradually declined to low levels at 72 hr in both SK-N-BE(2)c and KCN-69n neuroblastoma cell lines (Figures 1C and 1D). Analysis of HIF-2α protein levels at 1% O_2 revealed an almost opposite pattern. After an initial induction at 2 hr of hypoxia, HIF-2α protein levels increased over time and were upregulated after 72 hr in both analyzed neuroblastoma cell lines (Figures 1C and 1D). To mimic more physiological growth conditions with an oxygen pressure closer to that present in end capillaries, i.e., around 5% O_2 (Goda et al., 1997), we exposed neuroblastoma cells to 5% O_2 and analyzed HIF protein levels (Figures 1E and 1F). Whereas basal or induced HIF-1α protein was hardly detectable, a gradual and prominent increase over time in HIF-2α protein levels was seen in both cell lines, in agreement with the in vivo situation with high HIF-2α levels in well-oxygenated tumor areas. The steady-state levels of *HIF-1α* mRNA remained virtually unaffected (Figures 1G and 1H), while *HIF-2α* mRNA levels were upregulated at 1% and 5% O_2 in both cell lines (Figures 1I and 1J).

The differential changes over time of the HIF proteins at 1% O_2 and the seemingly efficient degradation of HIF-1α at 5% O_2 might reflect the expression levels of HIF-regulating PHDs under these conditions. In SK-N-BE(2)c (Figures 2A–2C) and KCN-69n (data not shown) cells, no consistent induction or reduction of *PHD1* mRNA levels was seen at either 21%, 5%, or 1% O_2. In contrast, as expected (Marxsen et al., 2004), a robust increase in *PHD2* and *PHD3* mRNA at both 5% and 1% O_2 was observed in both tested cell lines. PHD2 protein levels were induced at 1% O_2 in both tested cell lines, whereas no or limited induction was seen at 5% O_2 (Figures 2D–2G). Thus, despite the raise in *PHD2* and *PHD3* expression with time, HIF-2α protein increased at both 5% and 1% O_2, suggesting that HIF-2α is less sensitive to PHD2- and PHD3-induced degradation than HIF-1α is in neuroblastoma cells. Alternatively, as *HIF-2α* mRNA levels increase at 5% and 1% O_2, high de novo HIF-2α protein synthesis might counteract an increased PHD-induced degradation. Both HIF proteins were rapidly stabilized by the PHD inhibitors $CoCl_2$ and DIP (Figure S1). After 24 hr, HIF-1α protein was still present in cultures containing inhibitors, while HIF-2α protein in $CoCl_2$-treated cells decreased after 24 hr, in contrast to the sustained HIF-2α levels observed in DIP-treated and hypoxic cells (Figures S1A and S1B). As the *HIF-2α* mRNA levels increased in DIP- and $CoCl_2$-treated cells, but to a lesser extent in $CoCl_2$-treated cells (Figures S1C–S1F), it is possible that the high and sustained HIF-2α protein levels at hypoxia reflect the combined result of increased protein synthesis and less efficient protein degradation.

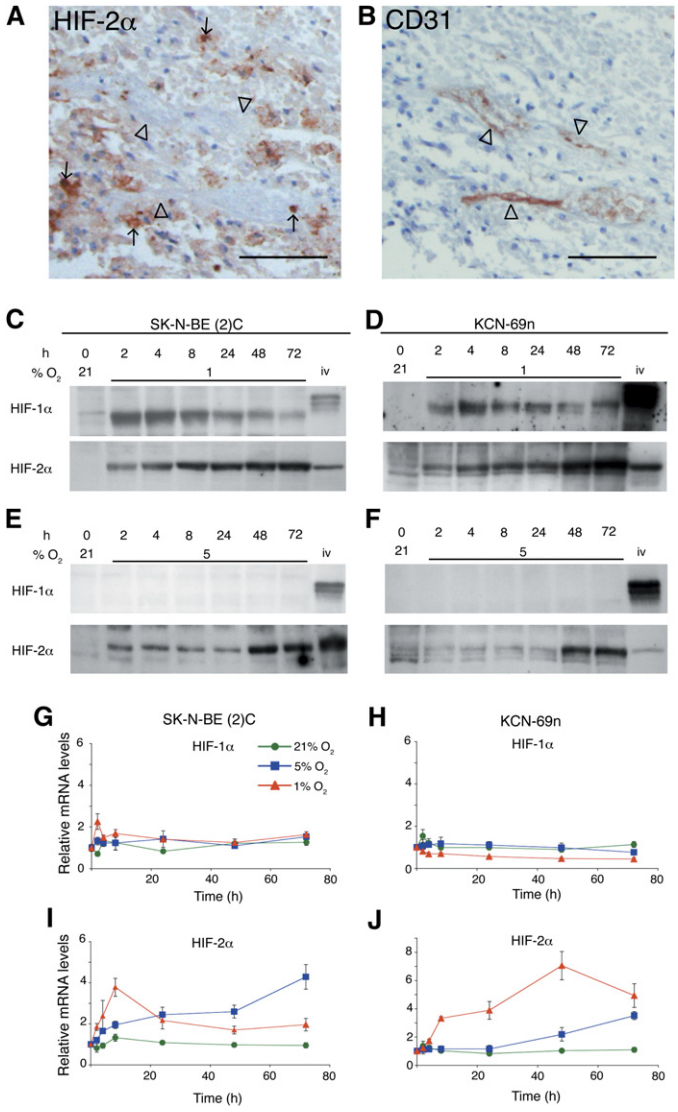

Figure 1. HIF-2α protein is present in well-vascularized neuroblastomas and in neuroblastoma cells cultured at physiological oxygen tensions

A and B: Immunohistochemical detection of nuclear HIF-2α (arrows, **A**) in well-vascularized areas of a stage 4 neuroblastoma specimen. CD31-positive vascular endothelial cells (arrowheads) are shown in a consecutive section (**B**). Scale bars, 100 μm.

C–J: HIF-1α and HIF-2α expression in neuroblastoma cells. **C–F:** Western blot analyses of changes in HIF-1α and HIF-2α protein levels in SK-N-BE(2)c and KCN-69n cells grown at either 1% (**C** and **D**) or 5% (**E** and **F**) O_2 for 0–72 hr. For comparison, HIF levels in cells grown at 21% O_2 are shown, and HIF-1α and HIF-2α in vitro translated (iv) proteins were used as positive controls. Representative results of three independent experiments are shown. **G–J:** Relative amounts of *HIF-1α* (**G** and **H**) and *HIF-2α* (**I** and **J**) mRNA, in SK-N-BE(2)c (**G** and **I**) and KCN-69n (**H** and **J**) cells as detected by Q-PCR. *HIF-1α* and *HIF-2α* mRNA levels are correlated to the expression of three reference genes (*SDHA*, *YWHAZ*, and *UBC*). Error bars denote the standard deviation within triplicates.

Subcellular localization and function of HIFs in neuroblastoma cells at 1% and 5% O_2

To evaluate the functional activity of HIF proteins at hypoxia and physiological oxygen tensions, we initially assessed their subcellular localization at 21%, 5%, or 1% O_2 in SK-N-BE(2)c cells. HIF-2α protein present at 21% O_2 was mainly detected in cytosolic extracts. At 5% O_2, induced HIF-2α was initially mainly

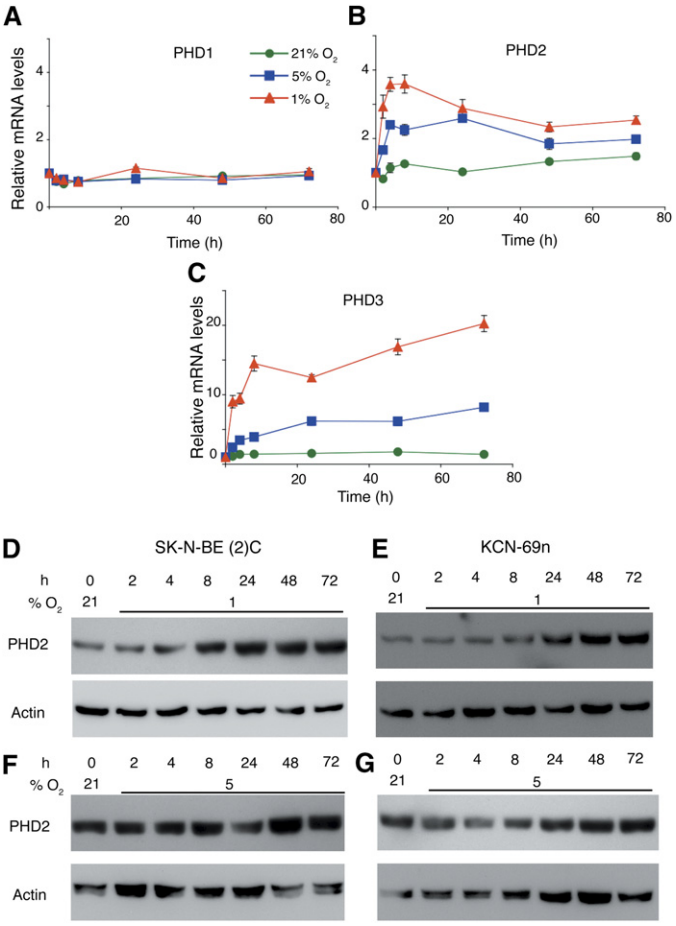

Figure 2. Kinetics of PHD mRNA and protein in neuroblastoma cells grown for 72 hr at 21%, 5%, or 1% O_2

A–C: Relative amounts of *PHD1*, *PHD2*, and *PHD3* mRNA in SK-N-BE(2)c cells were determined by Q-PCR and related to the mRNA levels of three reference genes (*SDHA*, *YWHAZ*, and *UBC*). Error bars show the standard deviation within triplicates.

D–G: PHD2 protein in SK-N-BE(2)c and KCN-69n cells cultured at 1% (**D** and **E**) and 5% (**F** and **G**) O_2. PHD2 levels at 21% O_2 are shown for comparison, and actin was used as a loading control. Data represent three independent experiments.

cytoplasmic, but after 72 hr most protein was accumulated in the nucleus (Figures 3A and 3B). As expected, no or small amounts of HIF-1α protein was detected at 21% or 5% O_2. In contrast, massive stabilization and nuclear localization of both HIF-1α and HIF-2α proteins were seen at 1% O_2 (Figures 3A and 3B). After 72 hr of growth, the small amount of HIF-1α protein detectable at 1% O_2 appeared to be nuclear.

HIF protein data at prolonged hypoxia and at 5% O_2 (Figures 1 and 3), and the fact that hypoxia-driven genes like *VEGF* and *DEC1/BHLHB2* are still expressed during chronic hypoxia (Jögi et al., 2002; Miyazaki et al., 2002), suggest that HIF-2α rather than HIF-1α is the major transcriptional regulator of prolonged hypoxic responses and that HIF-2α is active at physiological oxygen levels. The capacities of HIF-1α and HIF-2α to bind the HREs of the *VEGF* and *DEC1/BHLHB2* promoters at these conditions were tested by chromatin immunoprecipitation (ChIP) assays. The most robust binding of HIF-1α to the VEGF-HRE was detected after 4 hr at 1% O_2, whereas interaction with HIF-2α was most pronounced after 24 hr at 5% O_2 (Figure 3C).

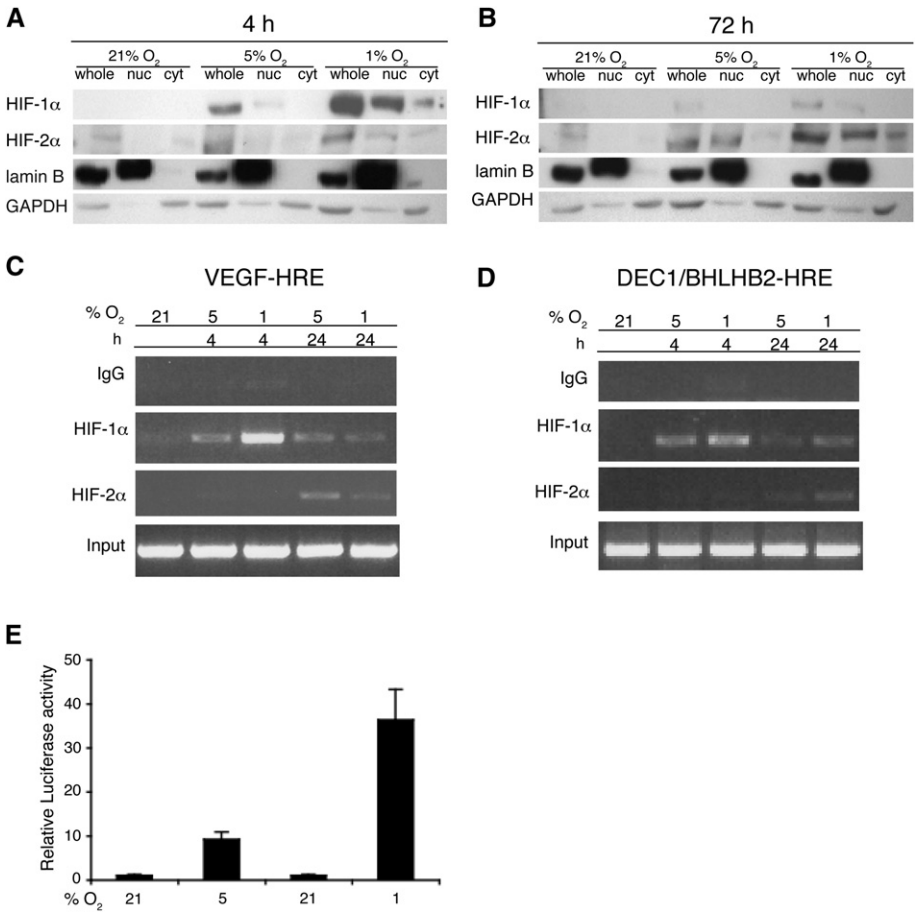

Figure 3. Subcellular localization and functional activity of HIF-1α and HIF-2α proteins in neuroblastoma cells

A and B: Whole-cell lysates (whole) and nuclei-enriched (nuc) and cytoplasmic (cyt) fractions of SK-N-BE(2)c cells were analyzed by immunoblotting. For relevant comparison, 60 μg of whole-cell protein lysates and the corresponding percentage of nuclear and cytoplasmic fractions were used for analysis. GAPDH and lamin B served as cytoplasmic and nuclear markers, respectively. Representative results of three independent experiments.

C and D: HIF-1α and HIF-2α binding to the *VEGF* and *DEC1/BHLHB2* promoters. ChIP assays on SK-N-BE(2)c cells exposed to 21%, 5%, or 1% O_2 for 4 and 24 hr. DNA was immunoprecipitated with anti-IgG control, anti-HIF-1α, or anti-HIF-2α antibodies, respectively. DNA was amplified by PCR, using primers flanking the VEGF-HRE and DEC1/BHLHB2-HRE, which generated amplicons of 275 and 166 bp, respectively. For input control, DNA from nonimmunoprecipitated extracts was used.

E: HRE transcriptional activity in neuroblastoma cells at 1% and 5% oxygen. SK-N-BE(2)c cells were transfected with a vector containing three copies of the EPO-HRE coupled to a Luciferase reporter gene. For reference, cells were cotransfected with a CMV Renilla Luciferase vector. Cells were cultured at 21, 5%, and 1% O_2 for 24 hr followed by measurements of Luciferase activity. Ratios between HRE and Renilla luciferase activities (HRE/CMV) were calculated and normalized to the control samples (21% O_2) in each experiment. Error bars show standard deviation of triplicate experiments.

Weak HIF-2α precipitates were also obtained at 4 hr at both 1% and 5% O_2. Binding of HIF-1α to the *VEGF* promoter could be detected in cells grown at 5% O_2 but was substantially reduced as compared to binding at 4 hr 1% O_2. A similar HIF-binding pattern was seen when analyzing occupancy of the DEC1/BHLHB2-HRE. Notably, HIF-2α binding was detected primarily at 24 hr (Figure 3D). In addition, neuroblastoma cells grown at 5% O_2 have the capacity to transcribe genes via HIF-binding HREs, as demonstrated in cells transfected with a vector containing three copies of the EPO-HRE coupled to a luciferase reporter gene (Figure 3E).

Gene induction at 1% and 5% oxygen correlates with differential regulation of HIF-α stability

As demonstrated previously (Jögi et al., 2002), and supported by data presented here, the overall response and adaptation to hypoxia are similar among neuroblastoma cell lines. A representative cell line for this response is SK-N-BE(2)c, and mRNA from these cells grown at 1%, 5%, and 21% O_2 for 0–72 hr was analyzed using microarray assays. Microarray expression data of *tyrosine hydroxylase* (*TH*) showed correlation to the HIF-1α and HIF-2α protein level patterns with regard to the rapid induction at 1% and the delayed upregulation at 5% O_2 (Figure 4A). These observations were independently validated using Q-PCR (Figure 4B). The *TH* expression pattern, representing an interesting data structure regardless of factual HIF dependence, was used as a template for further microarray data analyses. Genes with a similar microarray expression pattern were identified by calculating the projection length for each gene vector in the 1% O_2 series (n = 12,407; genes with valid expression data for all seven time points) onto the *TH* log2 expression vector (***TH 1% O_2***) (Figure S2A). Low absolute-valued projection lengths, centering on zero, were found to show no specific correlation to the *TH* vector. High projection lengths correlated well to the expression pattern of ***TH 1% O_2***, whereas the most extreme negative projection lengths were anticorrelated to ***TH 1% O_2***. By permuting the sample labels 1000 times and assaying projection length distribution in comparison to that of the observed data, a statistically significant projection length cut-off level was defined (Figure S2B). Genes having a projection length larger than 4.1 ($p = 0.040$) were considered significantly induced. These calculations gave a data set of 75 array reporters representing 64 known genes and five ESTs (Figure 5) with an expression pattern at 1% O_2 highly resembling that of *TH* (cf. Figures 4 and 5). Several of the identified genes have been demonstrated to be hypoxia responsive (Hu et al., 2003; Jögi et al., 2004; Semenza, 2003; Wenger et al., 2005). Using the TFASTA sequence comparison program, two ESTs were identified as the human endogenous retroviral genes *ERV3* (*ENR1_HUMAN*, $E = 1.1 \times 10^{-52}$) and *ENT1* (*ENT1_HUMAN*, $E = 3.2 \times 10^{-74}$). Some of the 64 genes have previously not been highlighted as being hypoxia driven, including *TRIO* and *SERPINB9*, both highly implicated in tumorigenesis and cell survival (van Houdt et al., 2005; Zheng et al., 2004). The early and sustained *TH* pattern seen at 1% O_2 was not significant for any group of genes at 5% or 21% O_2 (data not shown), but instead several of the 75

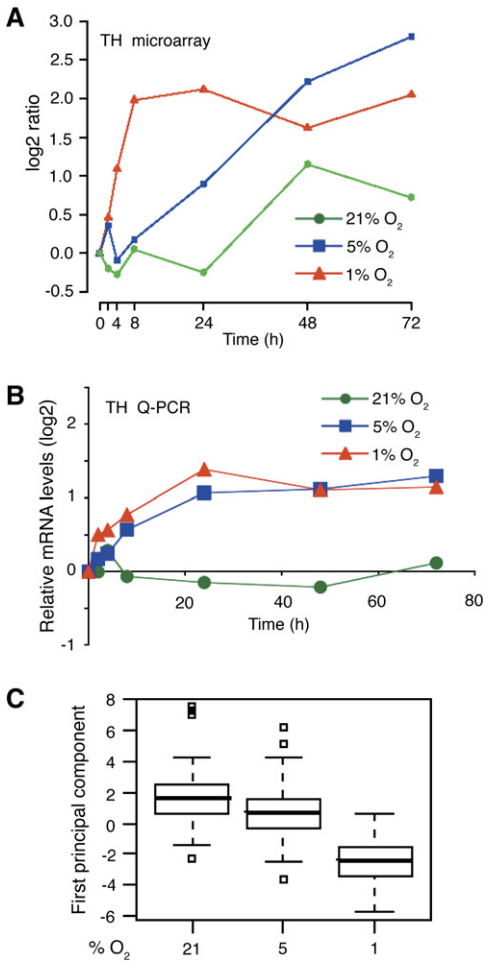

Figure 4. *TH* as a model gene for hypoxia-driven expression mimicking the stabilization patterns of HIF-1α and HIF-2α in neuroblastoma cells

A: *TH* mRNA levels in SK-N-BE(2)c cells grown at 1%, 5%, or 21% O_2 at indicated time points, as monitored by 70-mer oligonucleotide microarrays.

B: *TH* expression at corresponding oxygen levels and time points verified by Q-PCR, as related to the expression of three reference genes (*SDHA*, *YWHAZ*, and *UBC*).

C: Separation, using principal component analysis, of the 75 significantly induced genes, grouped by the three different oxygen levels. The median for each data set is indicated by the thick center line, and the first and third quartiles are the edges of the box. The brackets of the dashed vertical lines extending from the box show the last nonoutlier values, and points plotted individually represent potential outliers. The first principal component shown here described 83.2% of the variance in the data set. Groups were significantly different as determined by one-way ANOVA ($p < 0.001$) and Bonferroni-corrected pairwise Student's t tests ($p < 0.001$).

identified array reporters showed over time a slow increase in expression at 5% O_2 (Figure 5). Principal component analysis on the log2 ratio values followed by one-way ANOVA ($p < 0.001$) and Bonferroni-corrected pairwise Student's t tests ($p < 0.001$) between the oxygen treatment groups revealed that this was a general pattern among the 75 array reporters (Figure 4C). In summary, we demonstrate a strong, rapid, and significant induction of the identified genes at 1% O_2. In contrast, no significant induction was observed at 21% O_2. However, a slow induction was detected at 5% O_2, very similar to that documented for *TH* (cf. Figures 4 and 5). We confirmed this general expression pattern for a set of the 64 genes in two neuroblastoma cell lines using Q-PCR as exemplified by *DEC1/BHLHB2* and *NDRG1* (Figures 6A–6D).

HIF target genes differentially utilize HIF proteins at acute and prolonged hypoxia and at 5% O_2

To distinguish between HIF-1α- and HIF-2α-driven transcription, small inhibitory RNAs (siRNAs) against HIF-1α and HIF-2α were employed, focusing on the transcriptional activity of genes identified in our microarray analysis (Figure 5). We first confirmed a specific reduction of HIF mRNA and protein by cognate siRNA treatment at 4 and 24 hr at 1% O_2, and at 5% O_2 for 24 hr (Figures 7A, 7B, 7G, and 7H and Figure S3A). Upon acute (4 hr) hypoxic treatment, induced expression of *VEGF* and *DEC1/BHLHB2* was downregulated by siRNA against HIF-1α but not HIF-2α (Figures 7C and 7E). However, at prolonged hypoxia (1% O_2 for 24 hr) HIF-2α siRNA, in addition to HIF-1α siRNA, substantially reduced *VEGF* and *DEC1/BHLHB2* mRNA levels (Figures 7D and 7F). Taken together, our results strongly suggest that HIF-1α and HIF-2α act on the same genes but during different temporal windows, with HIF-1α primarily activated at the acute hypoxic phase and HIF-2α at later, prolonged stages of cellular adaptation to hypoxia.

The protein stabilization and subcellular localization data shown in Figures 1 and 3 in combination with the microarray analysis suggested that HIF-2α could be the dominant active HIF at 5% O_2. To directly test this notion, the expression levels of five selected genes identified in the microarray, *TH*, *VEGF*, *DEC1/BHLHB2*, *NDRG1*, and *SERPINB9*, were investigated in cells grown at 5% O_2 in the absence or presence of siRNA against either HIF-1α or HIF-2α. As shown in Figures 7I–7M, the expression of these genes was substantially reduced by HIF-2α siRNA. HIF-1α siRNA also reduced *TH*, *DEC1/BHLHB2*, and *NDRG1* expression, albeit with lower efficiency than siRNA against HIF-2α. Interestingly, *VEGF* and *SERPINB9* mRNA levels were virtually unaffected by HIF-1α siRNA at 5% O_2 but were clearly reduced by HIF-2α knockdown (Figures 7J and 7M). These results demonstrate that HIF-2α is actively regulating hypoxia-driven genes at physiological oxygen tensions. We also found that knockdown of either HIF-1α or HIF-2α reduced the mRNA levels of the glycolytic enzyme PGK1, indicating that HIF-2α can affect putative HIF-1α-specific target genes at physiological oxygen levels, at least in neuroblastoma cells (Figure 7N). However, not all genes induced at 5% O_2 appeared to be primarily regulated by HIF-2α, as exemplified by *BNIP3* (Figure 7O).

HIF-2α promotes an aggressive neuroblastoma phenotype

The specific effect of HIF-2α siRNA treatment on *VEGF* expression at 5% O_2, the known proangiogenic activity of VEGF, and the demonstrated correlation between blood vessel density and aggressiveness in many tumor forms (Carmeliet, 2005) prompted us to investigate if HIF-2α and VEGF were coexpressed in neuroblastoma specimens and whether HIF-2α protein is associated with an unfavorable outcome. Neuroblastoma specimens were immunohistochemically stained with anti-VEGF antibodies and screened for colocalization of VEGF and HIF-2α immunoreactivity in well-vascularized tumor areas, as defined by the presence of CD31-positive vascular endothelial cells. As illustrated in Figures 8A–8C, a strikingly concordant pattern of localized HIF-2α, VEGF, and CD31 immunoreactivity

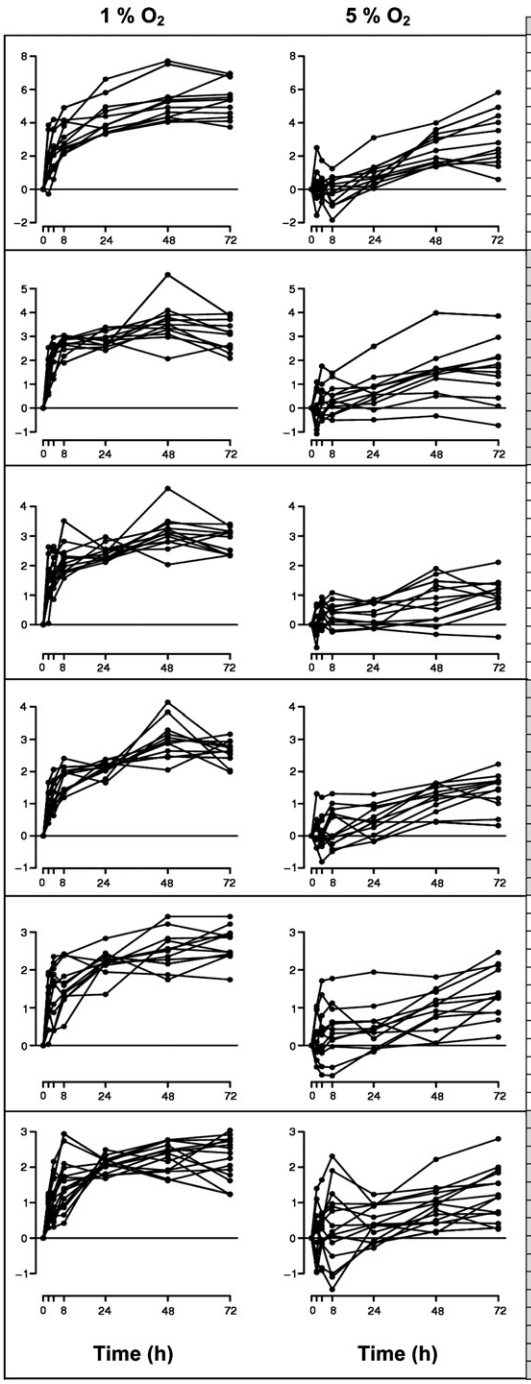

Rank	Genesymbol	Entrez GeneID
1	NDRG1	10397
2	LOC56901	56901
3	BHLHB2	8553
4	CRH	1392
5	VEGF	7422
6	PFKFB4	5210
7	KLK1	3816
8	ECFBP1	64168
9	DPY19L4	286148
10	*ENT1_HUMAN*	
11	VEGF	7422
12	SLC12A3	6559
13	TRIM29	23650
14	SART2	29940
15	ANKS1	23294
16	P4HA1	5033
17	JMJD1A	55818
18	PLOD2	5352
19	E2IG5	26355
20	AK3L1	205
21	CDH10	1008
22	STC1	6781
23	BNIP3	664
24	DDIT4	54541
25	SLC2A3	6515
26	C8orf58	541565
27	FLJ22374	84182
28	HK2	3099
29	BNIP3L	665
30	DEPDC6	64798
31	PPP1R3C	5507
32	SLC18A1	6570
33	PFKFB3	5209
34	CCNG2	901
35	AQP1	358
36	FLJ25967	440823
37	H300017799	
38	ADRB1	153
39	SLC17A1	6568
40	*ENR1_HUMAN*	
41	AK3L1	205
42	COX4I2	84701
43	ZNF395	55893
44	SERPINB9	5272
45	PAM	5066
46	SLC18A1	6570
47	FLJ22374	84182
48	OPN4	94233
49	MXI1	4601
50	STC2	8614
51	UTX	7403
52	CDC2L6	23097
53	HIST1H2AC	8334
54	H200016632	
55	RHOU	58480
56	C8orf44	56260
57	C1orf192	257177
58	TAS1R1	80835
59	H200004403	
60	C6orf170	221322
61	SYF2	25949
62	TRIO	7204
63	SP140	11262
64	SLC36A1	206358
65	JARID1B	10765
66	CPOX	1371
67	MERTK	10461
68	ZNF160	90338
69	PFAAP5	10443
70	LAYN	143903
71	ARHGEF6	9459
72	AQP10	89872
73	FLJ22374	84182
74	DNAJB4	11080
75	TH	7054

Figure 5. mRNA expression patterns for 75 significantly hypoxia-induced genes shown at 1% and 5% O_2

Genes were identified as hypoxia induced at 1% O_2 by calculation of projection length onto the target gene *TH*. Ranks are based on magnitude of calculated projection lengths in decreasing order. Entrez GeneID and Gene Symbol refer to the Entrez Gene database (Entrez Gene, http://www.ncbi.nih.gov/entrez/query.fcgi?db=gene). Genes with symbols in italics were identified using TFASTA and refer to Swiss-Prot (ExPASy-Swiss-Prot and TrEMBL, http://www.expasy.org/sprot/). Symbols for unidentified genes (starting with ''H …'') refer to the Oligo MicroArray Database (Operon) (Oligo MicroArray Database, OMAD, http://www.operon.com/arrays/omad.php?/). Genes are grouped for presentation purposes only.

was frequently observed. These data suggest that HIF-2α may drive the expression of VEGF and, hence, angiogenesis and tumor growth. To assess the importance of HIF-2α on tumor growth in vivo, neuroblastoma cells transiently transfected with siRNA against HIF-2α were injected into athymic mice. The time for tumor take did not significantly differ between the HIF-2α siRNA (4.3 ± 1.4 days) and control siRNA (4.6 ± 1.2 days) groups. However, strikingly, tumor growth was significantly impaired by targeting HIF-2α (Figure 8D). In contrast, transient knockdown of HIF-1α did not significantly affect xenograft tumor growth (Figure S3B).

To further investigate the in vivo effects of HIF-2α protein expression, we analyzed 93 primary neuroblastoma tumors arranged in a tissue microarray, addressing the hypothesis of local coexpression of HIF-2α and VEGF (cf. Figures 8A and 8B). We also analyzed whether HIF-2α levels could provide prognostic information regarding disease outcome. Tissue microarray sections, immunohistochemically stained for HIF-2α and VEGF, were scored as fractions of positive cells (range) as well as according to general intensity of positive cells. HIF-2α and VEGF correlated positively irrespective of whether range ($p < 0.001$) or intensity ($p = 0.009$) was used as the immunoreactivity

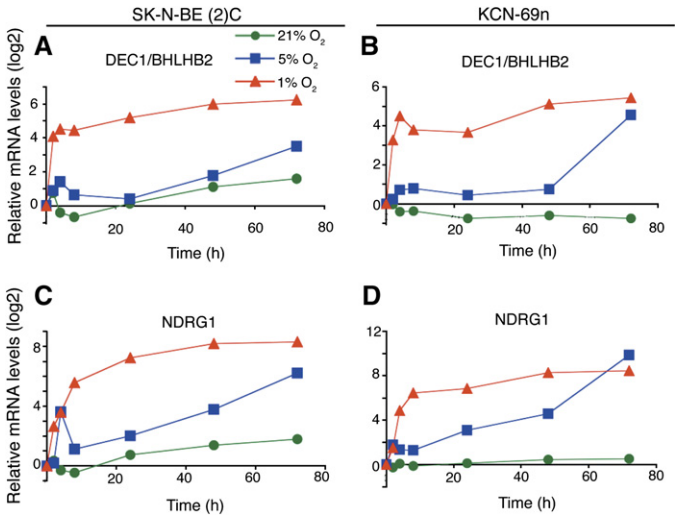

Figure 6. Verification by Q-PCR of the expression of two selected genes, which were identified by the microarray analysis and are correlated with the HIF stabilization and activity patterns at 1% and 5% oxygen

Expression levels of *DEC1/BHLHB2* (**A** and **B**) and *NDRG1* (**C** and **D**) were analyzed in SK-N-BE(2)c (**A** and **C**) and KCN-69n (**B** and **D**) cells grown at 21%, 5%, and 1% O_2 and related to the mRNA levels of three reference genes (*SDHA*, *YWHAZ*, and *UBC*).

measure (exemplified in Figure 8E). In addition, high HIF-2α intensity correlated significantly to high clinical stage ($p = 0.028$). To evaluate the prognostic significance of HIF-2α protein levels, Kaplan-Meier survival analysis was performed. A clear and significant difference in survival ($p = 0.004$) was seen, with high HIF-2α intensity predicting low overall survival (Figure 8F). A similar analysis for VEGF did not demonstrate a significant correlation to survival (data not shown), suggesting that HIF-2α affects tumor aggressiveness beyond the induction of VEGF expression. A further analysis of only the high-stage tumors (stages 3 and 4) revealed that HIF-2α intensity predicted survival also in this material ($p = 0.043$) (Figure 8G), making HIF-2α a prognostic marker independent of the clinical staging according to INSS (International Neuroblastoma Staging System). In conclusion, high levels of HIF-2α are associated with worse overall prognosis, and our results suggest that VEGF might be one of the downstream effectors contributing to this aggressive phenotype.

Discussion

HIF-1α has been directly or indirectly linked to the regulation of most investigated hypoxia-induced genes. The corresponding role of HIF-2α, on the other hand, is less clear (Park et al., 2003; Poellinger and Johnson, 2004; Takahashi et al., 2004). Gene elimination data indicate that HIF-2α function is required during development (Peng et al., 2000; Tian et al., 1998). In cancer, the HIF proteins are frequently coexpressed, thereby raising the questions of what their specific roles in growth and development of tumors are, and which genes are regulated by HIF-1α and by HIF-2α, respectively. Based on our data and the reported substantial redundancies in the utilization of the HIFs (Raval et al., 2005; Sowter et al., 2003; Warnecke et al., 2004), we argue that the answer lies not in which genes are transcribed by HIF-1α or HIF-2α, but rather in the conditions under which HIF-1α and

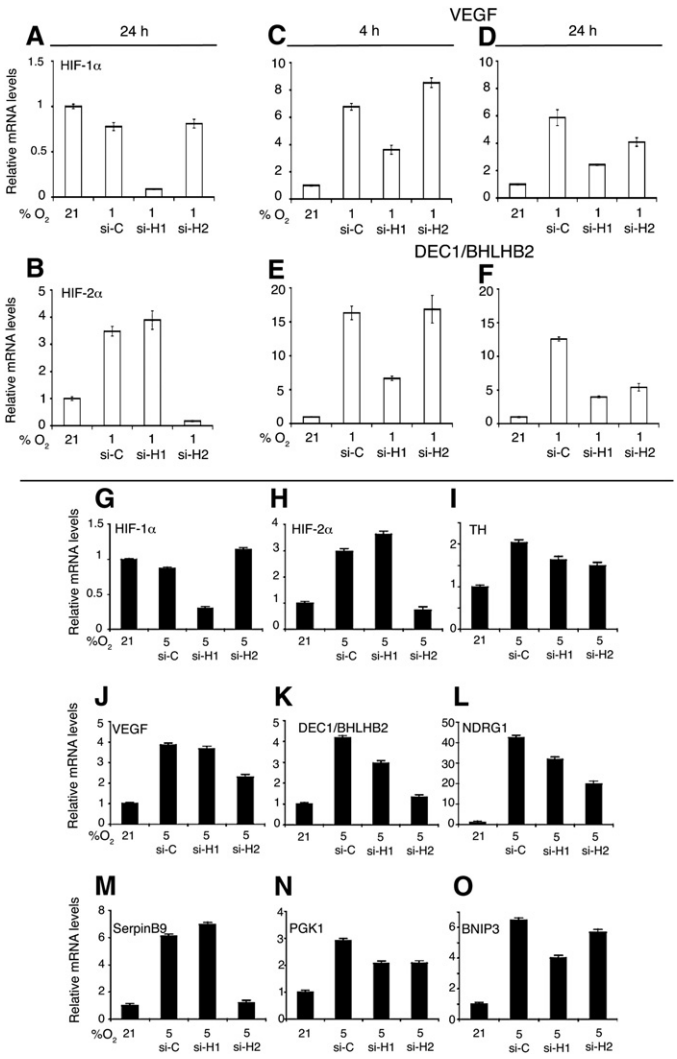

Figure 7. Differential utilization of HIF proteins in neuroblastoma cells depending on duration and severity of oxygen deprivation

Effects of selective siRNA treatment against HIF-1α and HIF-2α, respectively. SK-N-BE(2)c neuroblastoma cells were transfected at 21% O_2, and 16 hr after transfection, cultures were shifted to growth at 1% (**A–F**) or 5% (**G–O**) O_2. HIF mRNA expression (**A** and **B**) and expression of the known hypoxia-driven genes *VEGF* (**C** and **D**) and *DEC1/BHLHB2* (**E** and **F**), also identified in our microarray analysis, were analyzed at acute (4 hr) and prolonged (24 hr) hypoxia. **G–O**: HIF-2α regulates hypoxia-driven genes at physiological oxygen tensions in neuroblastoma cells. Expression of *HIF-1α* (**G**), *HIF-2α* (**H**), *TH* (**I**), *VEGF* (**J**), *DEC1/BHLHB2* (**K**), *NDRG1* (**L**), *SERPINB9* (**M**), *PGK1* (**N**), and *BNIP3* (**O**) was investigated in cells grown at 5% O_2 for 24 hr with or without siRNA against HIF-1α and HIF-2α, respectively. All mRNA levels were determined by Q-PCR analyses, and data were normalized to the expression of three reference genes (*SDHA*, *YWHAZ*, and *UBC*). An unspecific siRNA was used as control. Gene expression levels at 21% oxygen are shown for comparison. Error bars show the standard deviation within triplicates.

HIF-2α are stabilized, transcriptionally active, and subsequently utilized by hypoxia-regulated genes. We suggest that there is a temporal shift in HIF utilization, where HIF-1α is primarily active during the acute phase of hypoxic adaptation, and HIF-2α dominates during later, more chronic phases of hypoxia (Figure 8H). In addition, our data demonstrate that HIF-2α is also active at end capillary oxygen tensions, i.e., around 5% O_2. The finding that a number of classic hypoxia-driven genes can be transcribed by either HIF depending on the growth conditions might

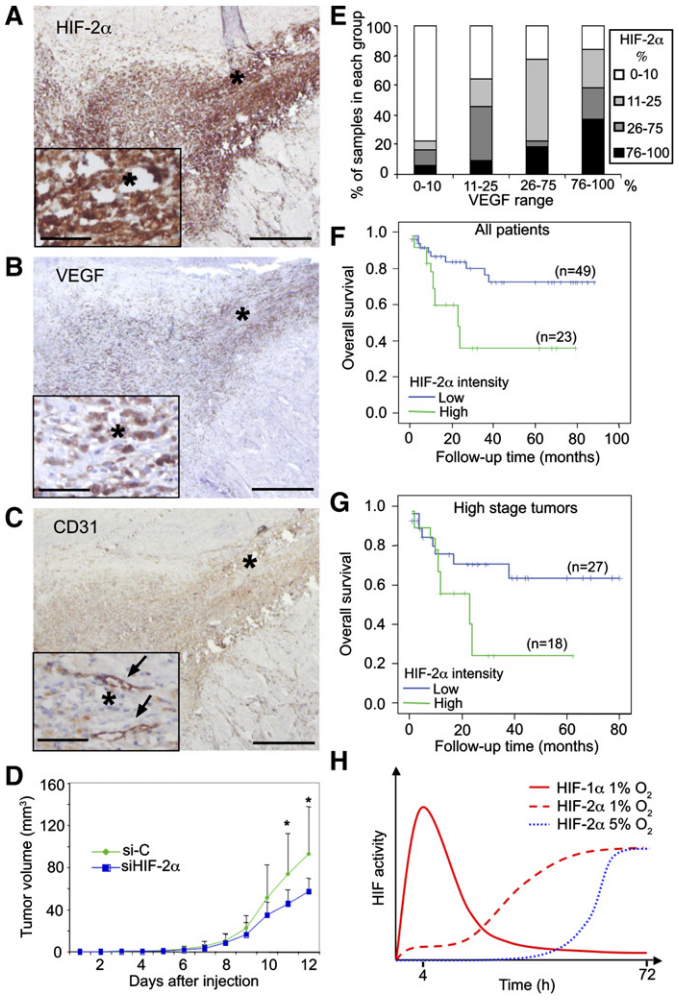

Figure 8. HIF-2α promotes an aggressive neuroblastoma phenotype

A–C: Immunohistochemical localization of HIF-2α (**A**), VEGF (**B**), and CD31 (**C**) in a stage 4 neuroblastoma tumor. Areas marked with asterisks are shown as insets in the respective panels, and the asterisks indicate the same position in the three consecutive sections. In **C**, arrows indicate blood vessels. Scale bars, 500 μm; scale bars in insets, 100 μm.

D: Reduced tumor growth in vivo by siRNA against HIF-2α. Xenograft experiment showing growth of SK-N-BE(2)c neuroblastoma cells, transfected with siRNA targeting HIF-2α (n = 15) or control (n = 15) in athymic mice. Tumor formation and volume were examined daily, and statistical significance was determined by Student's t test ($p < 0.05$). Error bars indicate SEM.

E: HIF-2α and VEGF immunoreactivities, assayed on a neuroblastoma tissue microarray, correlate positively as described by fraction of positive cells ($p < 0.001$, n = 81, Spearman correlation).

F: HIF-2α protein content predicts overall neuroblastoma patient survival ($p = 0.004$, n = 72, log rank test). HIF-2α intensity was scored in a four-grade scale on a tissue microarray, and scores were pooled into two groups: low (none and mild) and high (moderate and high) immunoreactivity.

G: HIF-2α protein content predicts survival of patients with high-stage (INSS stages 3 and 4) neuroblastoma ($p = 0.043$, n = 45, log rank test). HIF-2α intensity was scored as in **F**.

H: HIF-1α primarily governs acute hypoxic responses, whereas HIF-2α regulates gene expression under physiological oxygen conditions and at prolonged hypoxia. Model showing protein levels and activity of HIF-1α and HIF-2α at hypoxia (1% O_2) and HIF-2α under conditions close to end capillary oxygen levels (5% O_2) in neuroblastoma cells.

explain some diverging published data, as the differential temporal usage and oxygen sensitivity of the HIFs, so far, appear to have been largely overlooked.

As presented here, HIF-2α, in contrast to HIF-1α protein, is highly expressed in well-vascularized and apparently nonhypoxic lesions of the SNS-derived tumor neuroblastoma. These observations were corroborated by in vitro data showing that HIF-2α is stabilized and localized in the nucleus at physiological growth conditions (5% O_2) as well as at prolonged hypoxia (1% O_2). HIF-1α levels, on the other hand, were low at 5% O_2, especially in comparison to the levels at 1% O_2. Microarray data, together with the demonstrated binding of HIF-2α to the *VEGF* and *DEC1/BHLHB2* HREs in vivo and the selective downregulation of *VEGF* expression and other genes at 5% O_2 by HIF-2α siRNA, directly and unequivocally showed that HIF-2α is highly involved in regulation of classic hypoxia-driven genes at physiological oxygen tensions. One of these genes, *NDRG1*, is a known HIF-1α target but is induced at prolonged hypoxia in HIF-1α-negative cells (Cangul, 2004), supporting our hypothesis that HIF-2α governs gene regulation at chronic hypoxia. The expression of some of the investigated genes was also reduced by HIF-1α siRNA, showing that also HIF-1α can be active at physiological oxygen tensions, but interestingly, the induction of *VEGF* was seemingly unaffected by siRNA against HIF-1α at 5% O_2. The finding that *PGK1* expression is slightly regulated by HIF-2α at 5% oxygen is interesting, as *PGK1* has been shown to be a HIF-1α-driven gene in many cell systems (Covello et al., 2005; Dayan et al., 2006; Hu et al., 2003; Wang et al., 2005). Our results suggest that there are important differences in HIF usage between different cell types, although there are few studies that address the HIFs at near-physiological oxygen tensions. In support of our methodological approach, several of the genes identified by our time course microarray analysis have functional HREs (Semenza, 2003; Wenger et al., 2005) and showed slow upregulation at 5% O_2, establishing a general pattern as compared to the 1% and 21% O_2 series (Figure 4C). Among the genes showing this mode of regulation were *DEC1/BHLHB2*, *NDRG1*, *STC1*, and *VEGF*, all known to be induced by hypoxia and implicated in tumorigenic processes (Chakrabarti et al., 2004; Ryan et al., 1998; Wang et al., 2004; Yeung et al., 2005). In this group, we also identified several genes that have previously not been described as hypoxia responsive. Of significant interest were *TRIO* and *SERPINB9*. Amplification of *TRIO* in bladder neoplasms is associated with invasive and rapid growth, and when overexpressed in fetal kidney cells, *TRIO* increases tumorigenicity and invasiveness (Yoshizuka et al., 2004; Zheng et al., 2004). Overexpression of *SERPINB9* is associated with metastatic melanoma, and expression of this gene predicts poor prognosis in anaplastic large cell lymphoma (ten Berge et al., 2002; van Houdt et al., 2005). *SERPINB9* was also validated in our study as a HIF-2α-regulated gene at 5% oxygen. The human endogenous retroviral ERV3 protein has unknown functions but is normally expressed in the developing SNS (Andersson et al., 2002), adding to the list of hypoxia-regulated genes that support our previous finding that hypoxia drives neuroblastoma cells toward a neural crest-like stem cell phenotype (Jögi et al., 2002).

Hypoxia and activation of HIF-1α correlate with tumor progression and poor prognosis in several different cancers (Semenza, 2003). We show here that HIF-1α-driven genes can also be transcribed by HIF-2α at 5% O_2, suggesting that HIF-2α in neuroblastoma has the potential to act oncogenically at physiological oxygen levels as well as at prolonged hypoxia. Published data indicate that HIF-2α could exert the effects of

an oncogene (Covello et al., 2005; Kondo et al., 2003; Raval et al., 2005). However, HIF-2α, and HIF-1α as well, has been claimed to function as a tumor suppressor protein in glioblastoma and teratoma models (Acker et al., 2005). In that report and in agreement with our findings, overexpression of HIF-2α leads to increased VEGF expression and vascularization. In disagreement with our findings and the above-mentioned published data, the net effect of HIF-2α (and HIF-1α) overexpression on xenograft tumor growth was negative, presumably due to HIF-induced apoptosis. Apparently there are tissue-specific differences in response to high HIF protein levels (Blancher et al., 2000), although the Acker et al. data await confirmation in, for example, a larger and clinically characterized glioblastoma material, especially since VEGF and HIF-1α expression have been positively correlated to glioma progression (Jensen, 2006). In summary, HIF-2α activation is undoubtedly correlated with high tumor vascularization, and a role of HIF-2α in embryonal vascularization has been suggested (Peng et al., 2000). Here we show that preferentially HIF-2α and not HIF-1α mediates transcriptional activation of *VEGF* at physiological oxygen tensions. Accordingly, in a clinical neuroblastoma material there was a significant correlation between high VEGF and HIF-2α protein levels. Thus, there are strong implications for a direct involvement of HIF-2α in neuroblastoma angiogenesis, and our data suggest that this process could occur independently of pronounced hypoxia.

By knocking down HIF-2α in cultured neuroblastoma cells and subsequently injecting them subcutaneously in athymic mice, early growth of the resulting tumors was reduced, demonstrating an important role of HIF-2α in neuroblastoma growth. This result and the finding that high HIF-2α protein levels strongly predict adverse outcome in clinical neuroblastoma material provide compelling support for the involvement of HIF-2α in determining an aggressive neuroblastoma behavior. Importantly, our data also suggest that scoring HIF-2α protein levels in high-stage neuroblastomas will give direct prognostic information beyond that obtained by clinical staging. In addition, we show that HIF-2α can drive expression of genes involved in tumor migration and invasion, such as *SERPINB9*. In the clinical setting, this could lead to HIF-2α-dependent development of highly aggressive tumor cells also in less hypoxic tumor areas, contributing to the phenotypical heterogeneity frequently seen in neuroblastoma and in other solid tumors. Differences in the kinetics by which HIF-1α and HIF-2α proteins become accumulated at hypoxia have also been observed in HeLa, lung epithelial, and breast carcinoma cells (Holmquist et al., 2005; Uchida et al., 2004; Wiesener et al., 1998), suggesting that the HIF accumulation patterns seen here and a putative oncogenic role of HIF-2α are not unique to neuroblastomas. Taken together, we present evidence in support of a role of HIF-2α in neuroblastoma angiogenesis and growth, also under nonhypoxic conditions. The demonstration of differential HIF utilization under acute versus prolonged hypoxia further suggests that any HIF-related therapeutic strategies may benefit from selectively targeting either HIF-1α or HIF-2α.

Experimental procedures

Cell culture, western blot analysis, and quantitative real-time PCR

The SK-N-BE(2)c and KCN-69n human neuroblastoma cells were grown at reduced oxygen levels as described (Holmquist et al., 2005). For inhibition of PHD activity, cells were treated with 100 μM cobalt chloride ($CoCl_2$) or 200 μM 2,2′-dipyridyl (DIP). Western blotting and cellular fractionation were performed as described (Nilsson et al., 2005). Primary antibodies were as follows: anti-actin mAb (ICN Biomedicals), anti-HIF-1α and HIF-2α mAb (Novus Biologicals), anti-GAPDH mAb (Chemicon), anti-lamin B goat antiserum (Santa Cruz), and anti-PHD2 Ab (Novus). Horseradish peroxidase-conjugated secondary antibodies and Super Signal substrate (Pierce) were used for chemiluminescence detection.

RNA extraction, cDNA synthesis, and Q-PCR reactions with SYBR Green PCR master mix (Applied Biosystems) were performed as described (Löfstedt et al., 2004). Expression levels of genes of interest were normalized to the expression of three housekeeping genes (*SDHA*, *YWHAZ*, and *UBC*) not affected by reduced oxygen. Primers were designed using Primer Express (Applied), and sequences are given in Table S1.

Patient material and immunohistochemistry

Routinely fixed paraffin-embedded human neuroblastoma specimens (ethical approval LU 389-98, Lund University, Sweden) were analyzed by HIF-1α and HIF-2α immunohistochemistry. After antigen retrieval, HIF-2α (Novus), VEGF (Santa Cruz), and CD31 (Dako) immunoreactivities were detected using the Envision system and DAKO Techmate 500. A second neuroblastoma material consisting of 93 individual cases, selected based on tissue quality and availability, from patients diagnosed in Spain between 1998 and 2004, was arranged in a tissue microarray (ethical approval no. 59CI8ABR2002) and analyzed by HIF-2α and VEGF immunohistochemistry. Median age at diagnosis was 19 months, follow-up data were available for 79 patients, and follow-up time ranged between 1 and 88 months (S.N., R.N., E.F., and S.P., unpublished data). Forty samples were *MYCN* amplified, 53 were 1p36 deleted, and distribution in clinical stages (INSS) was as follows: stage 1 (19), stage 2 (5), stage 3 (13), stage 4 (39), stage 4s (7), and unclassified (10). High-stage, *MYCN*-amplified, and 1p36-deleted tumors were slightly overrepresented compared to a population-based distribution. Established prognostic markers, e.g., clinical stage, *MYCN* amplification, and 1p36 deletion were all prognostically highly significant in this material (data not shown). Immunoreactivity was independently scored by two pathologists and classified according to range, i.e., fractions of positive cells (0, 0%–10%; 1, 10%–25%; 2, 26%–75%; 3, 76%–100%) and general intensity of positive cells (0, none; 1, mild; 2, moderate; 3, intense). For survival analysis and correlation to stage, groups 0 and 1 (low) and 2 and 3 (high) were pooled, respectively. All statistical calculations were performed using SPSS 12.0.1 (SPSS Inc.).

Microarray analysis

mRNA from SK-N-BE(2)c cells grown at 1%, 5%, or 21% O_2 were hybridized to microarrays (~27,000 unique clones) produced at the Swegene DNA Microarray Resource Center, Lund University. Genes with a specific response pattern were identified using a vector projection method onto a given trend of interest. Data analyses and statistical computations were performed using BASE (Saal et al., 2002), Perl (http://www.perl.org/), and R (http://www.r-project.org/). Identification of unknown array reporters was done using TFASTA. See the Supplemental Experimental Procedures for a detailed description of microarray platform and analyses.

ChIP assay

Cells were cultured at 21% O_2 or reduced oxygen, and ChIP analyses were performed as previously described (Löfstedt et al., 2004), using antibodies against HIF-1α (Santa Cruz), HIF-2α (Novus), or IgG (Abcam). PCR primers flanking the HREs of the *VEGF* and *DEC1/BHLHB2* promoters are given in Table S1.

Transfection, luciferase assay, and siRNA

Triplicates of 8×10^4 SK-N-BE(2)c cells in 24-well culture plates were transfected with 300 ng of a vector containing three copies of the erythropoietin (EPO) HRE in tandem, coupled to a Luciferase reporter gene (Kallio et al., 1999; Löfstedt et al., 2004). As a control of transfection efficiency, 50 ng of a CMV Renilla Luciferase vector (Promega) was included. Transfections were performed with Lipofectamine-2000 for 6 hr in OptiMEM I Reduced Serum Medium (Invitrogen), and cells were harvested after 24 hr of culture at indicated oxygen levels. The luciferase activity was measured and calculated using the Dual-Luciferase Reporter Assay System (Promega). In a set of

experiments, cells were transfected with siRNA duplexes (Ambion) against HIF-1α and HIF-2α, respectively, at a final concentration of 50 nM. As control siRNAs, the inverted or a scrambled HIF-1α sequence were used. Sense and antisense siRNA sequences are given in Table S1 and have been previously described (Sowter et al., 2003).

Xenograft tumor model

SK-N-BE(2)c cells were transiently transfected with HIF-2α, HIF-1α, or scrambled (control) siRNA. Cells were injected subcutaneously (5×10^6 cells/200 μl PBS/mouse) on the back of athymic mice (NMRI strain nu/nu). Six- to eight-week-old female mice weighing 20–25 g at arrival were used and housed in a controlled environment. All procedures were approved by the regional ethical committee for animal research (approval no. M66-05). Tumor growth was monitored on a daily basis, and volume was calculated as $\pi ls^2/6$, where l = long side and s = short side.

Supplemental data

The Supplemental Data include Supplemental Experimental Procedures, three supplemental figures, and one supplemental table and can be found with this article online at http://www.cancercell.org/cgi/content/full/10/5/413/DC1/.

Acknowledgments

We thank Mrs. Siv Beckman for skillful technical assistance. This work was supported by the Swedish Cancer Society, the Children's Cancer Foundation of Sweden, the Swedish Research Council, HKH Kronprinsessan Lovisas Förening för Barnasjukvård, Hans von Kantzows Stiftelse, the Swedish Foundation for Strategic Research, the Research Programme in Medical Bioinformatics of the Swedish Knowledge Foundation, the Knut and Alice Wallenberg Foundation via the Swegene program, the research funds of Malmö University Hospital, the European Union, and grants G03/089 and PI 05/0383 from Instituto Carlos III, Madrid, Spain.

Received: December 23, 2005
Revised: May 30, 2006
Accepted: August 29, 2006
Published: November 13, 2006

References

Acker, T., Diez-Juan, A., Aragones, J., Tjwa, M., Brusselmans, K., Moons, L., Fukumura, D., Moreno-Murciano, M.P., Herbert, J.M., Burger, A., et al. (2005). Genetic evidence for a tumor suppressor role of HIF-2α. Cancer Cell *8*, 131–141.

Andersson, A.C., Venables, P.J., Tonjes, R.R., Scherer, J., Eriksson, L., and Larsson, E. (2002). Developmental expression of HERV-R (ERV3) and HERV-K in human tissue. Virology *297*, 220–225.

Blancher, C., Moore, J.W., Talks, K.L., Houlbrook, S., and Harris, A.L. (2000). Relationship of hypoxia-inducible factor (HIF)-1α and HIF-2α expression to vascular endothelial growth factor induction and hypoxia survival in human breast cancer cell lines. Cancer Res. *60*, 7106–7113.

Brown, J.M., and Wilson, W.R. (2004). Exploiting tumour hypoxia in cancer treatment. Nat. Rev. Cancer *4*, 437–447.

Cangul, H. (2004). Hypoxia upregulates the expression of the NDRG1 gene leading to its overexpression in various human cancers. BMC Genet. *5*, 27.

Carmeliet, P. (2005). VEGF as a key mediator of angiogenesis in cancer. Oncology *69* (*Suppl. 3*), 4–10.

Chakrabarti, J., Turley, H., Campo, L., Han, C., Harris, A.L., Gatter, K.C., and Fox, S.B. (2004). The transcription factor DEC1 (stra13, SHARP2) is associated with the hypoxic response and high tumour grade in human breast cancers. Br. J. Cancer *91*, 954–958.

Covello, K.L., Simon, M.C., and Keith, B. (2005). Targeted replacement of hypoxia-inducible factor-1α by a hypoxia-inducible factor-2α knock-in allele promotes tumor growth. Cancer Res. *65*, 2277–2286.

Covello, K.L., Kehler, J., Yu, H., Gordan, J.D., Arsham, A.M., Hu, C.J., Labosky, P.A., Simon, M.C., and Keith, B. (2006). HIF-2α regulates Oct-4: Effects of hypoxia on stem cell function, embryonic development, and tumor growth. Genes Dev. *20*, 557–570.

Dayan, F., Roux, D., Brahimi-Horn, M.C., Pouyssegur, J., and Mazure, N.M. (2006). The oxygen sensor factor-inhibiting hypoxia-inducible factor-1 controls expression of distinct genes through the bifunctional transcriptional character of hypoxia-inducible factor-1α. Cancer Res. *66*, 3688–3698.

Epstein, A.C., Gleadle, J.M., McNeill, L.A., Hewitson, K.S., O'Rourke, J., Mole, D.R., Mukherji, M., Metzen, E., Wilson, M.I., Dhanda, A., et al. (2001). C. elegans EGL-9 and mammalian homologs define a family of dioxygenases that regulate HIF by prolyl hydroxylation. Cell *107*, 43–54.

Goda, F., O'Hara, J.A., Liu, K.J., Rhodes, E.S., Dunn, J.F., and Swartz, H.M. (1997). Comparisons of measurements of pO_2 in tissue in vivo by EPR oximetry and microelectrodes. Adv. Exp. Med. Biol. *411*, 543–549.

Harris, A.L. (2002). Hypoxia—A key regulatory factor in tumour growth. Nat. Rev. Cancer *2*, 38–47.

Höckel, M., and Vaupel, P. (2001). Tumor hypoxia: Definitions and current clinical, biologic, and molecular aspects. JNCI Cancer Spectrum. J. Natl. Cancer Inst. *93*, 266–276.

Hoehner, J.C., Gestblom, C., Hedborg, F., Sandstedt, B., Olsen, L., and Påhlman, S. (1996). A developmental model of neuroblastoma: Differentiating stroma-poor tumors' progress along an extra-adrenal chromaffin lineage. Lab. Invest. *75*, 659–675.

Holmquist, L., Jögi, A., and Påhlman, S. (2005). Phenotypic persistence after reoxygenation of hypoxic neuroblastoma cells. Int. J. Cancer *116*, 218–225.

Hu, C.J., Wang, L.Y., Chodosh, L.A., Keith, B., and Simon, M.C. (2003). Differential roles of hypoxia-inducible factor 1α (HIF-1α) and HIF-2α in hypoxic gene regulation. Mol. Cell. Biol. *23*, 9361–9374.

Huang, L.E., Gu, J., Schau, M., and Bunn, H.F. (1998). Regulation of hypoxia-inducible factor 1α is mediated by an O_2-dependent degradation domain via the ubiquitin-proteasome pathway. Proc. Natl. Acad. Sci. USA *95*, 7987–7992.

Iyer, N.V., Kotch, L.E., Agani, F., Leung, S.W., Laughner, E., Wenger, R.H., Gassmann, M., Gearhart, J.D., Lawler, A.M., Yu, A.Y., and Semenza, G.L. (1998). Cellular and developmental control of O_2 homeostasis by hypoxia-inducible factor 1α. Genes Dev. *12*, 149–162.

Jain, S., Maltepe, E., Lu, M.M., Simon, C., and Bradfield, C.A. (1998). Expression of ARNT, ARNT2, HIF1α, HIF2α and Ah receptor mRNAs in the developing mouse. Mech. Dev. *73*, 117–123.

Jensen, R.L. (2006). Hypoxia in the tumorigenesis of gliomas and as a potential target for therapeutic measures. Neurosurg. Focus *20*, E24.

Jögi, A., Øra, I., Nilsson, H., Lindeheim, A., Makino, Y., Poellinger, L., Axelson, H., and Påhlman, S. (2002). Hypoxia alters gene expression in human neuroblastoma cells toward an immature and neural crest-like phenotype. Proc. Natl. Acad. Sci. USA *99*, 7021–7026.

Jögi, A., Vallon-Christersson, J., Holmquist, L., Axelson, H., Borg, Å., and Påhlman, S. (2004). Human neuroblastoma cells exposed to hypoxia: Induction of genes associated with growth, survival, and aggressive behavior. Exp. Cell Res. *295*, 469–487.

Kallio, P.J., Wilson, W.J., O'Brien, S., Makino, Y., and Poellinger, L. (1999). Regulation of the hypoxia-inducible transcription factor 1α by the ubiquitin-proteasome pathway. J. Biol. Chem. *274*, 6519–6525.

Kondo, K., Kim, W.Y., Lechpammer, M., and Kaelin, W.G., Jr. (2003). Inhibition of HIF2α is sufficient to suppress pVHL-defective tumor growth. PLoS Biol. *1*, E83 10.1371/journal.pbio.0000083.

Lando, D., Peet, D.J., Whelan, D.A., Gorman, J.J., and Whitelaw, M.L. (2002). Asparagine hydroxylation of the HIF transactivation domain a hypoxic switch. Science *295*, 858–861.

Löfstedt, T., Jögi, A., Sigvardsson, M., Gradin, K., Poellinger, L., Påhlman, S., and Axelson, H. (2004). Induction of ID2 expression by hypoxia-inducible factor-1: A role in dedifferentiation of hypoxic neuroblastoma cells. J. Biol. Chem. *279*, 39223–39231.

Mahon, P.C., Hirota, K., and Semenza, G.L. (2001). FIH-1: A novel protein that interacts with HIF-1α and VHL to mediate repression of HIF-1 transcriptional activity. Genes Dev. *15*, 2675–2686.

Marxsen, J.H., Stengel, P., Doege, K., Heikkinen, P., Jokilehto, T., Wagner, T., Jelkmann, W., Jaakkola, P., and Metzen, E. (2004). Hypoxia-inducible factor-1 (HIF-1) promotes its degradation by induction of HIF-α-prolyl-4-hydroxylases. Biochem. J. *381*, 761–767.

Miyazaki, K., Kawamoto, T., Tanimoto, K., Nishiyama, M., Honda, H., and Kato, Y. (2002). Identification of functional hypoxia response elements in the promoter region of the DEC1 and DEC2 genes. J. Biol. Chem. *277*, 47014–47021.

Nilsson, H., Jögi, A., Beckman, S., Harris, A.L., Poellinger, L., and Påhlman, S. (2005). HIF-2α expression in human fetal paraganglia and neuroblastoma: Relation to sympathetic differentiation, glucose deficiency, and hypoxia. Exp. Cell Res. *303*, 447–456.

Park, S.K., Dadak, A.M., Haase, V.H., Fontana, L., Giaccia, A.J., and Johnson, R.S. (2003). Hypoxia-induced gene expression occurs solely through the action of hypoxia-inducible factor 1α (HIF-1α): Role of cytoplasmic trapping of HIF-2α. Mol. Cell. Biol. *23*, 4959–4971.

Peng, J., Zhang, L., Drysdale, L., and Fong, G.H. (2000). The transcription factor EPAS-1/hypoxia-inducible factor 2α plays an important role in vascular remodeling. Proc. Natl. Acad. Sci. USA *97*, 8386–8391.

Petrella, B.L., Lohi, J., and Brinckerhoff, C.E. (2005). Identification of membrane type-1 matrix metalloproteinase as a target of hypoxia-inducible factor-2α in von Hippel-Lindau renal cell carcinoma. Oncogene *24*, 1043–1052.

Poellinger, L., and Johnson, R.S. (2004). HIF-1 and hypoxic response: The plot thickens. Curr. Opin. Genet. Dev. *14*, 81–85.

Raval, R.R., Lau, K.W., Tran, M.G., Sowter, H.M., Mandriota, S.J., Li, J.L., Pugh, C.W., Maxwell, P.H., Harris, A.L., and Ratcliffe, P.J. (2005). Contrasting properties of hypoxia-inducible factor 1 (HIF-1) and HIF-2 in von Hippel-Lindau-associated renal cell carcinoma. Mol. Cell. Biol. *25*, 5675–5686.

Ryan, H.E., Lo, J., and Johnson, R.S. (1998). HIF-1α is required for solid tumor formation and embryonic vascularization. EMBO J. *17*, 3005–3015.

Saal, L.H., Troein, C., Vallon-Christersson, J., Gruvberger, S., Borg, Å., and Peterson, C. (2002). BioArray Software Environment (BASE): A platform for comprehensive management and analysis of microarray data. Genome Biol. *3*, SOFTWARE0003.

Sato, M., Tanaka, T., Maemura, K., Uchiyama, T., Sato, H., Maeno, T., Suga, T., Iso, T., Ohyama, Y., Arai, M., et al. (2004). The PAI-1 gene as a direct target of endothelial PAS domain protein-1 in adenocarcinoma A549 cells. Am. J. Respir. Cell Mol. Biol. *31*, 209–215.

Semenza, G.L. (2003). Targeting HIF-1 for cancer therapy. Nat. Rev. Cancer *3*, 721–732.

Sowter, H.M., Raval, R.R., Moore, J.W., Ratcliffe, P.J., and Harris, A.L. (2003). Predominant role of hypoxia-inducible transcription factor (Hif)-1α versus Hif-2α in regulation of the transcriptional response to hypoxia. Cancer Res. *63*, 6130–6134.

Takahashi, R., Kobayashi, C., Kondo, Y., Nakatani, Y., Kudo, I., Kunimoto, M., Imura, N., and Hara, S. (2004). Subcellular localization and regulation of hypoxia-inducible factor-2α in vascular endothelial cells. Biochem. Biophys. Res. Commun. *317*, 84–91.

Talks, K.L., Turley, H., Gatter, K.C., Maxwell, P.H., Pugh, C.W., Ratcliffe, P.J., and Harris, A.L. (2000). The expression and distribution of the hypoxia-inducible factors HIF-1α and HIF-2α in normal human tissues, cancers, and tumor-associated macrophages. Am. J. Pathol. *157*, 411–421.

ten Berge, R.L., Meijer, C.J., Dukers, D.F., Kummer, J.A., Bladergroen, B.A., Vos, W., Hack, C.E., Ossenkoppele, G.J., and Oudejans, J.J. (2002). Expression levels of apoptosis-related proteins predict clinical outcome in anaplastic large cell lymphoma. Blood *99*, 4540–4546.

Tian, H., Hammer, R.E., Matsumoto, A.M., Russell, D.W., and McKnight, S.L. (1998). The hypoxia-responsive transcription factor EPAS1 is essential for catecholamine homeostasis and protection against heart failure during embryonic development. Genes Dev. *12*, 3320–3324.

Uchida, T., Rossignol, F., Matthay, M.A., Mounier, R., Couette, S., Clottes, E., and Clerici, C. (2004). Prolonged hypoxia differentially regulates hypoxia-inducible factor (HIF)-1α and HIF-2α expression in lung epithelial cells: Implication of natural antisense HIF-1α. J. Biol. Chem. *279*, 14871–14878.

van Houdt, I.S., Oudejans, J.J., van den Eertwegh, A.J., Baars, A., Vos, W., Bladergroen, B.A., Rimoldi, D., Muris, J.J., Hooijberg, E., Gundy, C.M., et al. (2005). Expression of the apoptosis inhibitor protease inhibitor 9 predicts clinical outcome in vaccinated patients with stage III and IV melanoma. Clin. Cancer Res. *11*, 6400–6407.

Wang, Z., Wang, F., Wang, W.Q., Gao, Q., Wei, W.L., Yang, Y., and Wang, G.Y. (2004). Correlation of N-myc downstream-regulated gene 1 overexpression with progressive growth of colorectal neoplasm. World J. Gastroenterol. *10*, 550–554.

Wang, V., Davis, D.A., Haque, M., Huang, L.E., and Yarchoan, R. (2005). Differential gene up-regulation by hypoxia-inducible factor-1α and hypoxia-inducible factor-2α in HEK293T cells. Cancer Res. *65*, 3299–3306.

Warnecke, C., Zaborowska, Z., Kurreck, J., Erdmann, V.A., Frei, U., Wiesener, M., and Eckardt, K.U. (2004). Differentiating the functional role of hypoxia-inducible factor (HIF)-1α and HIF-2α (EPAS-1) by the use of RNA interference: Erythropoietin is a HIF-2α target gene in Hep3B and Kelly cells. FASEB J. *18*, 1462–1464.

Wei, J.S., Greer, B.T., Westermann, F., Steinberg, S.M., Son, C.G., Chen, Q.R., Whiteford, C.C., Bilke, S., Krasnoselsky, A.L., Cenacchi, N., et al. (2004). Prediction of clinical outcome using gene expression profiling and artificial neural networks for patients with neuroblastoma. Cancer Res. *64*, 6883–6891.

Wenger, R.H., Stiehl, D.P., and Camenisch, G. (2005). Integration of oxygen signaling at the consensus HRE. Sci. STKE *2005*, re12.

Wiesener, M.S., Turley, H., Allen, W.E., Willam, C., Eckardt, K.U., Talks, K.L., Wood, S.M., Gatter, K.C., Harris, A.L., Pugh, C.W., et al. (1998). Induction of endothelial PAS domain protein-1 by hypoxia: Characterization and comparison with hypoxia-inducible factor-1α. Blood *92*, 2260–2268.

Wiesener, M.S., Jurgensen, J.S., Rosenberger, C., Scholze, C.K., Horstrup, J.H., Warnecke, C., Mandriota, S., Bechmann, I., Frei, U.A., Pugh, C.W., et al. (2003). Widespread hypoxia-inducible expression of HIF-2α in distinct cell populations of different organs. FASEB J. *17*, 271–273.

Yeung, H.Y., Lai, K.P., Chan, H.Y., Mak, N.K., Wagner, G.F., and Wong, C.K. (2005). Hypoxia-inducible factor-1-mediated activation of stanniocalcin-1 in human cancer cells. Endocrinology *146*, 4951–4960.

Yoshizuka, N., Moriuchi, R., Mori, T., Yamada, K., Hasegawa, S., Maeda, T., Shimada, T., Yamada, Y., Kamihira, S., Tomonaga, M., and Katamine, S. (2004). An alternative transcript derived from the trio locus encodes a guanosine nucleotide exchange factor with mouse cell-transforming potential. J. Biol. Chem. *279*, 43998–44004.

Zheng, M., Simon, R., Mirlacher, M., Maurer, R., Gasser, T., Forster, T., Diener, P.A., Mihatsch, M.J., Sauter, G., and Schraml, P. (2004). TRIO amplification and abundant mRNA expression is associated with invasive tumor growth and rapid tumor cell proliferation in urinary bladder cancer. Am. J. Pathol. *165*, 63–69.

Accession numbers

The microarray raw data are available in MIAME compliant format from the ArrayExpress database (http://www.ebi.ac.uk/arrayexpress/) with accession number E-MEXP-836.